Planetary and Space Science 121 (2016) 1–9

Contents lists available at ScienceDirect

Planetary and Space Science

journal homepage: www.elsevier.com/locate/pss

InSight coordinates determination from direct-to-Earth radio-tracking and Mars topography model

Le Maistre Sebastien *

Jet Propulsion Laboratory, California Institute of Technology, 4800 Oak Grove Dr, Pasadena 91109, California, USA

ARTICLE INFO

Article history:
Received 23 September 2015
Accepted 4 November 2015
Available online 19 December 2015

Keywords:
Lander coordinate
Mars
Direct-to-Earth Doppler
Topography

ABSTRACT

The InSight mission is planned to land on the surface of Mars in September 2016. Close to the equator in Elysium Planitia, in the vicinity of the Curiosity location, the exact landing site coordinates cannot be provided by the navigation team. The direct-to-Earth (DTE) Doppler measurements are rarely included in the early lander localization process since DTE Doppler cannot provide the *Z*-coordinate (along the polar axis) with a precision better than a few kilometers after a few days of operation. Most of the recent landers used two-way UHF Doppler with Odyssey to determine the inertial location of the lander quickly. Sometimes the lander location is also provided from imaging using triangulation techniques. However, there is no InSight commitment to use UHF Doppler nor images taken from InSight camera to locate the lander. If DTE Doppler data are not suitable to determine the *Z*-coordinate of InSight, these data are very powerful to rapidly estimate the in-equatorial plane coordinates with high precision. The present study proposes, tests and quantifies a new method to determine *Z* much faster and more precisely than from DTE Doppler data only. The method consists of inferring the *Z*-coordinate from the accurate estimates of the in-equatorial plane coordinates and from the current topography model of Mars. We show that our method will allow us estimating InSight's *Z*-coordinate within ± 10 m or better depending on the topography model used and on the actual lander location: the flatter and the higher in latitude, the better. This is two orders of magnitude more precise than the DTE Doppler solution and at least 5 times more precise than the triangulated lander location from imaging. The possible bias in the *Z* estimate of InSight with the proposed method is shown to likely be insignificant based on the application of the method onto the previous landed missions.

1. Introduction

The NASA mission InSight (Interior Exploration using Seismic Investigations, Geodesy and Heat Transport) is scheduled for a March 2016 launch date and set to arrive on the surface of Mars in September 2016. It will send a lander to the Martian surface relying on proven technologies used on NASA's Mars Phoenix mission. The lander will nominally spend two Earth years investigating the deep interior of Mars and the processes that shaped the rocky planets of the inner solar system (including Earth) more than four billion years ago. This mission, comprising a seismometer and a heat flow probe, also holds the Rotation and Interior Structure Experiment (RISE) using the spacecraft communication system to provide precise measurements of planetary rotation (Folkner et al., 2012). The RISE data will also be used to determine the lander coordinates. There is no mission requirements to estimate the lander location, but a precise knowledge of it will certainly improve the quality of the science analysis (for instance by making easier the recognition of the geological features seen on the lander's pictures) and allow high resolution cameras from spacecraft like MRO to correctly target the lander.

Although radio tracking data are commonly used to determine the lander coordinates, it is also well known that the direct-to-Earth Doppler data are not suitable for a precise estimate of the *Z*-coordinate (height above the equator) of the landed probe (see e.g. Le Maistre et al., 2012). To compensate this lack of sensitivity of the DTE Doppler tracking data, the MERs benefited from high resolution images on which the landed probes were visible (Kuchynka et al., 2014), the Phoenix mission availed of an additional UHF Doppler link to Mars Odyssey, and Pathfinder and the Viking landers used extra range to DSN (Deep Space Network) measurements. The latter data typically give the distance lander-DSN station at the few meters level. This helpful information to position the lander with respect to Earth loses power when projected in the Mars centered reference frame since it correlates

* Tel.: +1 818 354 4381.
E-mail address: Sebastien.Le.Maistre@jpl.nasa.gov

http://dx.doi.org/10.1016/j.pss.2015.11.003

with the Mars ephemeris errors. InSight will have UHF telemetry primarily to MRO, but no UHF Doppler will be used to locate the lander since it affects MRO's data rate. No range to DSN will be performed for InSight because InSight uses a Medium Gain Antenna (MGA) (against High Gain Antenna (HGA) for Viking landers and Mars Pathfinder) for which the Signal-to-Noise Ratio (SNR) would be too much degraded. With the camera on its arm, InSight could also take panoramic images to be used to locate the lander relative to surface features observed in images such as CTX and HiRISE. The absolute cartographic accuracy of the controlled photomosaics, tied to MOLA, is 50 m (1σ, pers. com. T. Duxbury). Such a method would allow the camera team to quickly determine the position of the lander, without DTE Doppler and ranging. This localization was completed within 1 day for Pathfinder, Spirit and Opportunity. However, there is no project commitment when such InSight camera images would be taken and therefore there could be a location ambiguity early after landing. This is the reason why the approach presented here could be required for a location solution within days after InSight landing.

This paper proposes a new method to rapidly determine all three position coordinates of InSight. We show in this study how precise will be the determination of the *Z*-coordinate if estimated from (1) the in-equatorial plane coordinates obtained very quickly (few days) and precisely (meter level) from the DTE Doppler data and from (2) the current topography model of Mars surface derived from MGS MOLA.

For a better understanding of the paper, let us first set the definitions of the confusing terms used throughout this paper:

- *Precision* refers to how much variation or dispersion exists from the average (mean), or estimated value. This can also be denoted as the standard deviation, or 1σ formal error, or uncertainty as well as the range of possible values or error bar.
- *Accuracy* refers to the difference between the estimated value and the actual value of a given parameter (true error).

2. DTE Doppler data to estimate the lander coordinates

The DTE radiotracking data are commonly used to determine the coordinates of landers and rovers at the surface of Mars (Folkner et al., 1997; Kuchynka et al., 2014). These data consist of two-way Doppler[1] measurements between a ground station on Earth and the landed probe. The ground station transmits a high frequency (S- or X-band) signal, which is coherently (i.e. with no phase shift) sent back to Earth by the lander through the onboard telecom system (transponder and antennas). By nature, the Doppler data are highly sensitive to the radial position variations and insensitive to variations perpendicular to the Line Of Sight (LOS). Le Maistre et al. (2012) have quantified the precision as a function of time with which the cartesian coordinates of an equatorial lander can be determined only based on two-way X-band DTE Doppler data. They showed in particular that *X* and *Y* (the in-equatorial plane coordinates) are estimated at the meter level after 2 tracking passes of about one hour each, whereas *Z* uncertainty remains as large as a couple of kilometers and barely improve to a hundred of meters after one martian year of weekly tracking. The poor sensitivity of the DTE Doppler to any variations along the *Z*-axis, resulting in $\sigma_Z \simeq 1000\sigma_X$, is explained by the small ($\pm 30^\circ$) and slow (annual) variations of the angle between the *Z*-direction and the LOS-direction around 90°. On the contrary, the equatorial plane coordinates are rapidly determined because of a favorable Doppler geometry: the angle between the *X*- and *Y*- direction of a rotating frame tied to the planet and the LOS-direction is much faster and larger, with daily events of (quasi) maximum sensitivity (when Earth sets and rises in the lander's sky).

Table 1
Order of magnitude of the lander coordinates precision (1σ) obtained by analyzing the two-way X-band DTE Doppler data. The numbers are picked up from Le Maistre et al. (2012). The first line reports the a priori uncertainties used by these authors.

Time-span	σ_{X_0}	σ_{Y_0}	σ_{Z_0}	σ_{r_0}	σ_{λ_0}
A priori	200 km	200 km	200 km	200 km	$\sim 3.5^\circ$
2 days	1 m	1 m	3 km	1 m	$\leq 10^{-4\circ}$
700 days	10 cm	10 cm	100 m	10 cm	$\leq 10^{-5\circ}$

The precisions obtained by Le Maistre et al. (2012) are summarized in Table 1 for the two particular cases of coordinates estimated after 2 days and after 700 days (about the nominal mission duration of InSight). The table gives 1σ uncertainties (or precisions) both in cartesian and cylindrical systems. In the rest of the paper we focus on the cylindrical coordinate system (r, λ, Z), which is the one used in the literature to provide the coordinates of the previous landed probes (Folkner et al., 1997; Kuchynka et al., 2014).

Since the goal of our method is to provide information about the lander location at the beginning of the mission, we consider herein as the nominal scenario, a situation where an a priori knowledge on the lander location would be the one we have after two days of DTE tracking (see Table 1).

3. The topography model of Mars

The topography model used in the present study is a plate model DSK (Digital Shape Kernel) set produced by the JPL-NAIF team. The DSKs are created from MGS laser altimeter (MOLA, Smith et al., 2001) 128 pixel/deg digital elevation model (DEM). This corresponds to a resolution of $\sim$0.5 km/pixel close to the equator. This source data set covers the latitude range 87S:87N and can be found at http://pds-geosciences.wustl.edu/mgs/mgs-m-mola-5-megdr-l3-v1/mgsl_300x/meg128. The DEMs are converted to plate models using custom, prototype software. Plates were produced by joining the DEM surface points corresponding to adjacent pixel centers. Each set of four adjacent centers gives rise to two plates. The large surface regions covered by the DEMs are broken up into smaller regions in the DSK file set. Coverage of the DSK files provides a 1/2 pixel overlap at the coverage boundaries. The nominal arrangement of the vertices of the DSK set is such that the horizontal coordinates of the vertices correspond to the horizontal coordinates of the DEM pixel centers. So the projections of the non-hypotenuse plate edges onto a sphere have nominal angular measures of 1/128°. Due to height variations, the average non-hypotenuse plate edge length will be somewhat longer than the average projection.

The DSKs have been validated by the NAIF team using another custom, prototype program. This program checked that the original DEM heights at pixel centers could be recovered with high accuracy from the DSKs. Only spot checks have been performed to compare interpolated heights from the DEMs and the DSKs. These showed widespread agreement at the sub-meter level, but some differences are at the 100 m level. These large differences probably should be expected, due to the steep Mars terrain and large size of the DEM pixels. Visit the http://naif.jpl.nasa.gov/pub/naif/misc/alpha_dsk_N0064/ website for more information about SPICE-DSK models.

[1] In theory, range data could be used too, but this will not be the case for InSight as mention in Section 1.

4. InSight landing site

InSight will land in western Elysium Planitia on Hesperian plains about 540 km north of the Curiosity landing site. The favored landing ellipse (called E09) is centered at about 4.4° north latitude and 136° east longitude just north of the dichotomy boundary (Golombek et al., 2014). The 3σ (99%) landing error ellipse is 130×27 km. Fig. 1 shows the topography model at two different spatial-scales both centered on the landing ellipse. In the landing site area of InSight, the topography model resolution is on average $\sim$0.5 km since the terrain height variations are small.

5. Method

Basically, the idea is extremely simple: using the topography model, we infer Z and its error bar from the estimates (solutions and uncertainties) of the longitude (λ) and distance to spin axis (r) as provided by the DTE radio-tracking data. For this analysis, we assume that the DTE Doppler will provide: $\lambda_0 \pm \sigma_{\lambda_0}, r_0 \pm \sigma_{r_0}$ and $Z_0 \pm \sigma_{Z_0}$, where the σ's order of magnitudes are reported in Table 1. The method amounts considering a representative set of $\lambda_i \in \lambda_0 \pm \sigma_{\lambda_0}$ for which we compute the coordinates of the points $P_i = (r_i, \lambda_i, Z_i)$ laid on the surface defined by the topography model. Then, we keep each $Z_i \in Z_0 \pm \sigma_{Z_0}$ for which the distance to spin axis r_i is within $r_0 \pm \sigma_{r_0}$. This provides us a reduced range of allowed Z-coordinate for that lander, as shown in red in Fig. 2. This is a direct approach to propagate the small uncertainties in λ_0, r_0 into Z, considered to be a priori known with a large uncertainty (σ_{Z_0}).

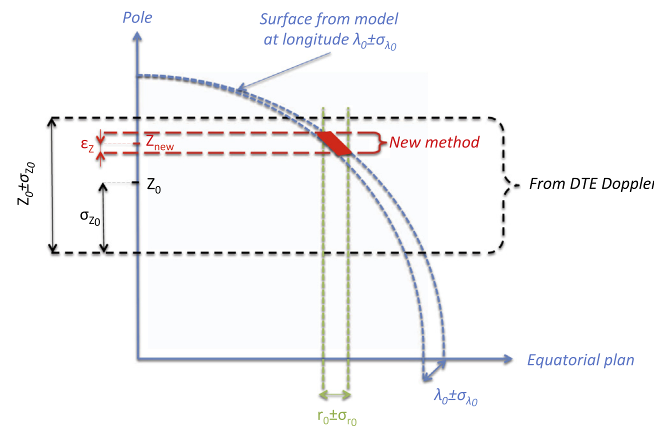

Fig. 2. Scheme explaining the method. (For interpretation of the references to color in this figure caption, the reader is referred to the web version of this paper.)

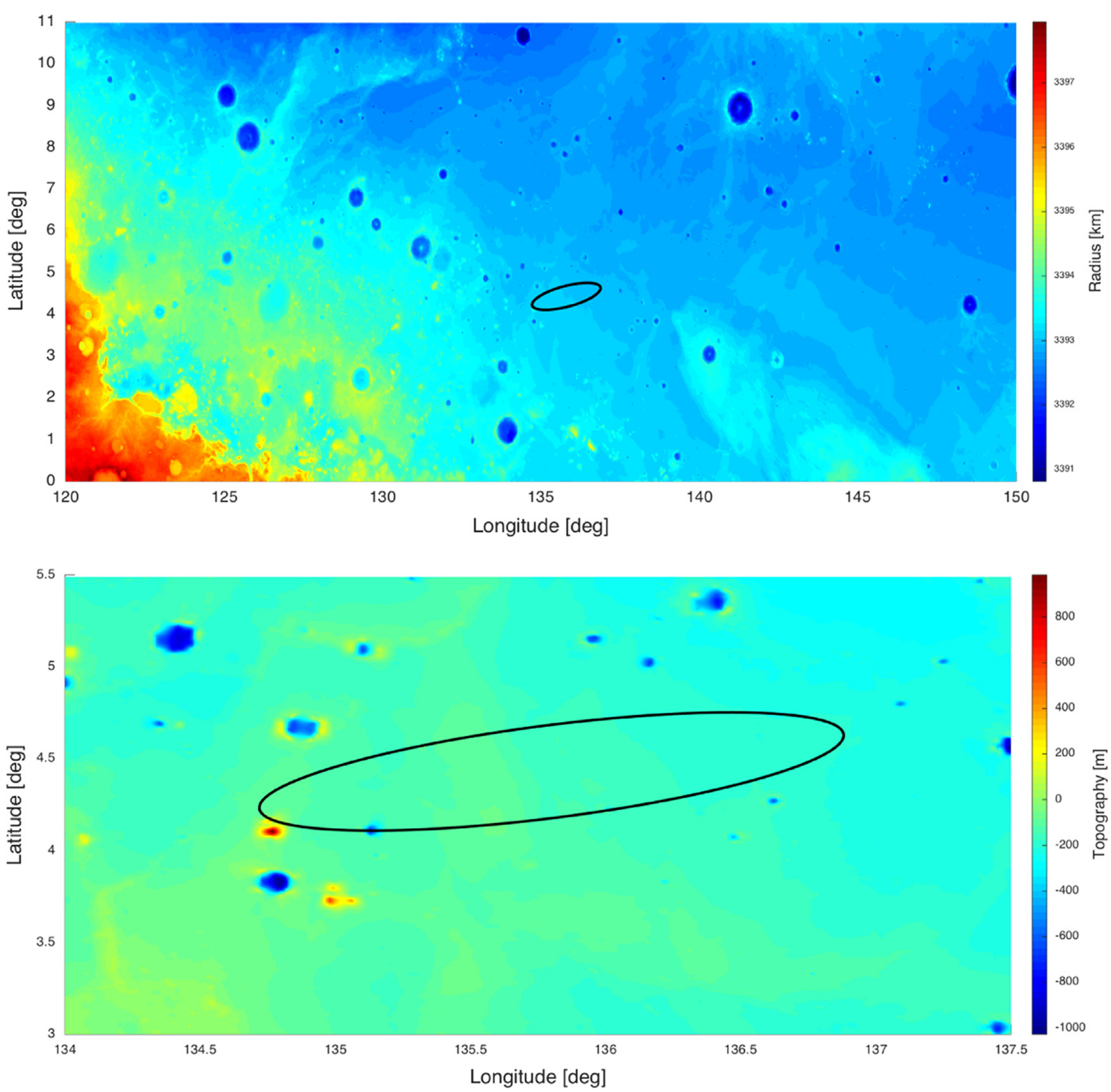

Fig. 1. Mars Topography in the region of the landing ellipse of InSight as provided by the JPL-NAIF DSK model.

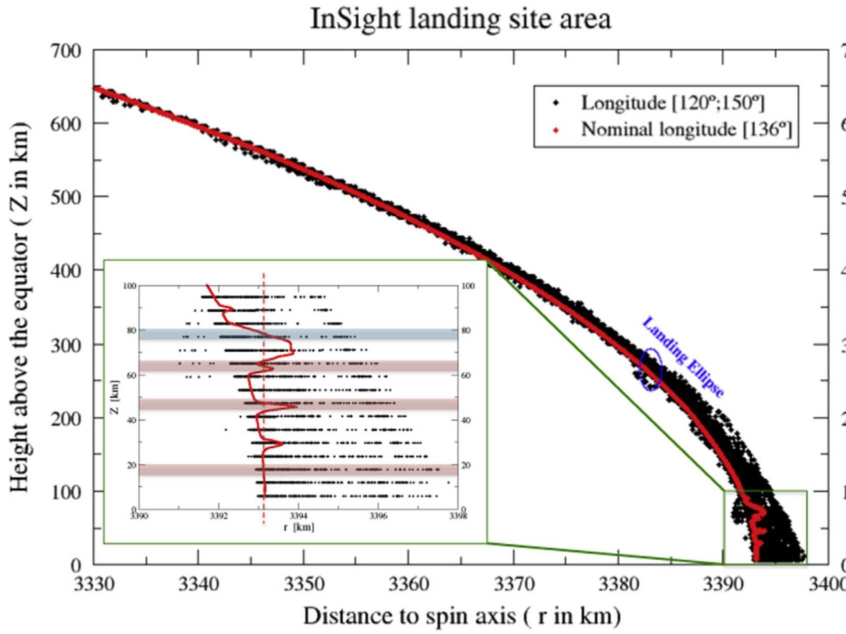

Fig. 3. *Z*-coordinate as a function of the distance to spin axis *r* in a range of 0°:11° of latitude. The green framed zone is zoomed in the bottom-left of the graph and shows how oddly *Z* and *r* can evolved for a given longitude (λ). As an example, the vertical red dashed line points out when crossing the solid red curve how many *Z* correspond to the arbitrary chosen r=3393.1 km even when considering only one given longitude, here $\lambda = 136^\circ$ (solid red). The thickness of the four horizontal boxes corresponds to the uncertainty area provided by the Doppler estimates of *Z* (i.e. $\pm\sigma_{Z_0} = 3$ km). Blue box shows an example of where our method would work and the red boxes show where it would fail to reduce the *Z* uncertainty (σ_{Z_0}). (For interpretation of the references to color in this figure caption, the reader is referred to the web version of this paper.)

Note that without this a priori constraints on the allowed range of Z_i, the method could suffer from many ambiguities. Indeed, due to the ellipsoidal shape of Mars and its topography, several *Z*-coordinates (at least two, one in each hemisphere) correspond to one given pair of longitude and distance to spin axis (λ, r). However, since the navigation team provides a reduced elliptic area where the lander is ensured to be, the Mars ellipsoidal shape ambiguity is unlikely in general and not a problem for InSight. But the hills, valleys, craters, pits and cliffs could still bring some ambiguities. If not accounted for, such ambiguities could in turn be responsible for large bias on *Z* when inferring the latter from an accurate knowledge of λ and *r*. As shown in Fig. 3 the probability for having such an ambiguous determination is (in the landing range of longitude) higher at lower latitude than it is in the landing ellipse of InSight. As a worse case example, with a topography as the one pointed out with the solid red curve in the bottom-left frame of Fig. 3 and with an hypothetical landing ellipse centered on $\lambda = 136^\circ$ and Z=40 km, the method proposed could not improve the uncertainty on *Z* coming from the ellipse dimension (i.e. $\sigma_Z \simeq 30$ km) unless by taking into account the low-precision solution obtained with the DTE Doppler data (i.e. $\sigma_{Z_0} = 3$ km, see Table 1). And even with this additional DTE information, our method could fail to reduce the uncertainty on *Z* (σ_{Z_0}) given the actual location of the lander. The red boxes in Fig. 3 are examples of failure, whereas the blue box shows in the same hypothetical ellipse a location for which the method would be powerful. Fortunately, the failure cases of this worse scenario is unlikely to correspond to the real case of InSight, since the later is planned to land in a flat-smooth area, where the method is proven below to be precise and (likely) accurate.

6. InSight location uncertainty map

In this section we predict the precision with which the *Z*-coordinate of InSight will be estimated with our method depending on its actual location in the landing ellipse. To do so, the method described above is applied at every surface point[2] $P_i = (\phi_i, \lambda_i)$ of the grid overlaying the landing region with a step arbitrarily chosen equal to 0.02° in both latitude (ϕ) and longitude (λ). The set of selected *Z* so obtained for each P_i allows us to compute the "range" and the uncertainty in Z_i. The latter assumes a Gaussian distribution of *Z*s which is not the case most of the time, whereas the former correspond to the difference between the maximum and the minimum value of allowed *Z*. This range in *Z*, which can be seen as twice the error bar (ε_{Z_i}) associated to Z_i given our knowledge on λ and *r*, is more representative of the precision we should get on Z_i than the standard deviation (σ_{Z_i}) named uncertainty herein. Nevertheless, both the ranges and the uncertainties predicted by our method for the nominal scenario (i.e. after 2 days of DTE Doppler tracking) are plotted in Fig. 4 upper and lower panels, respectively. We see on that figure that almost every spot of the landing ellipse should allow the determination of Z from λ and *r* in a range of about 20 m, i.e. with an error bar of about $\varepsilon_Z = 10$ m. This realistic precision is about 10 times worse than the $\sigma_Z \simeq 1$ m we get in most of the spots in the northern part of the ellipse as shown on the lower panel of Fig. 4. Because of the presence on the ellipse border of some major edifices (craters and hills in the South-West region, see Fig. 1), an unfortunate landing in this unlikely zone would make us unable to provide a more precise estimate of *Z* than that provided by the Doppler.

To be confident with the precision on *Z* we get with our method, we assessed the impact of the a priori knowledge σ_{λ_0} and σ_{r_0} on the range of selected *Z* as a function of the lander location. We found that estimating the longitude of the lander 10 times more precisely (i.e. with $\sigma_{\lambda_0} = 10^{-5\circ}$) would provide very similar precision on *Z* than with $\sigma_{\lambda_0} = 10^{-4\circ}$, whereas degrading it by a factor of 10 (i.e. with $\sigma_{\lambda_0} = 10^{-3\circ}$) would increase the range of selected *Z* by about 1 m (i.e. ~10%), which is also quite few. On the other hand, an increase of the uncertainty in *r* by a factor of 10 (i.e. with $\sigma_{r_0} = 10$ m) would increase the error bars on *Z* by a factor of 2 (i.e. adding 10 m to the nominal $\varepsilon_Z = 10$ m for the error bar), but such a low precision in *r* is very unlikely for InSight.

[2] The P_i's are the landing location candidates.

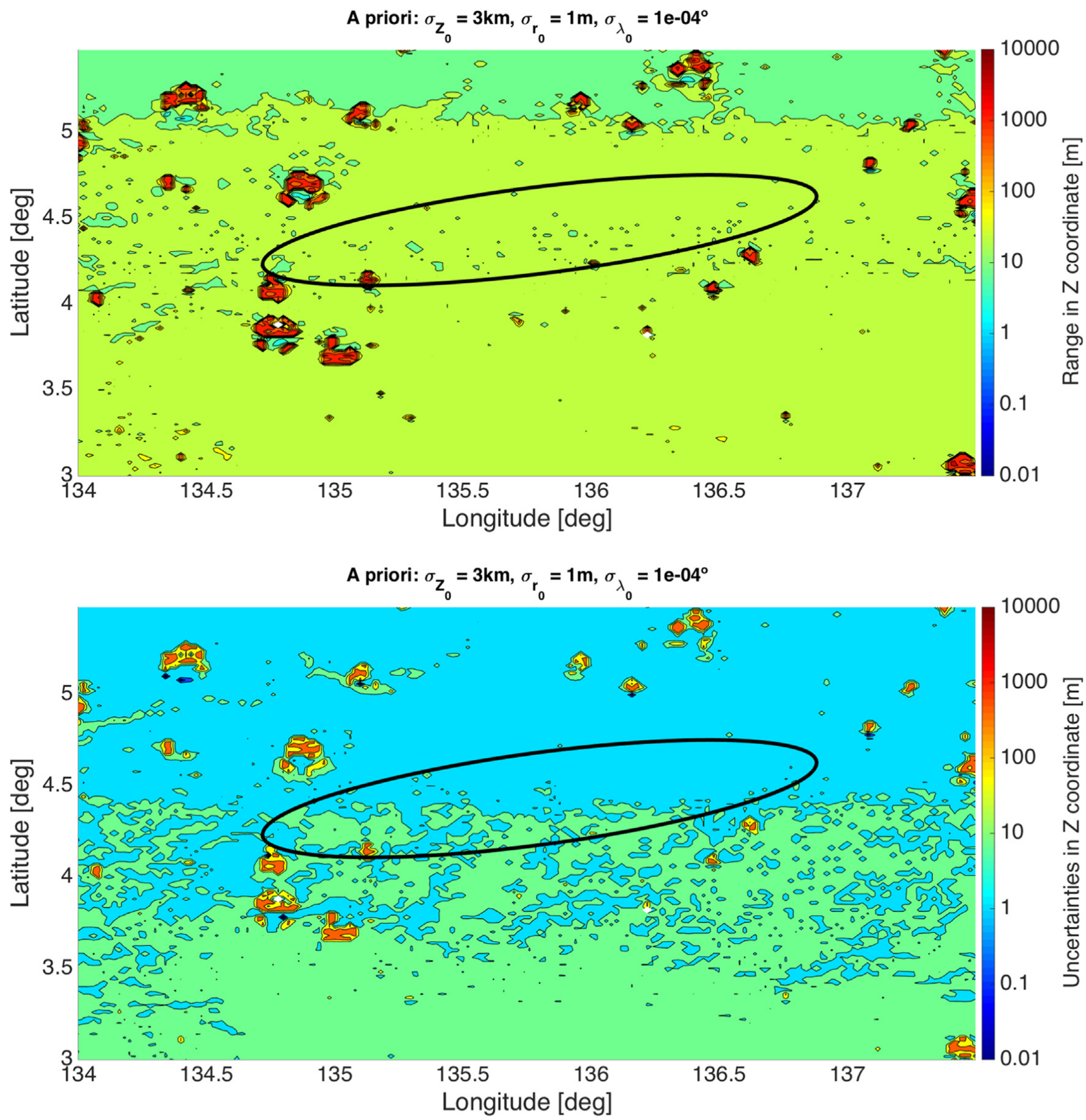

Fig. 4. Range (upper panel) and uncertainties (lower panel) in *Z*-coordinates as a function of the actual lander location inferred from a priori knowledge that we get after two days of DTE Doppler tracking of InSight.

Generally speaking, the uncertainty in Z depends weakly on the uncertainty in λ but strongly depends on σ_{r_0}. Indeed, a Δr variation will induce a ΔZ variation of same amplitude, since the relation between r and Z in the landing ellipse is almost linear with a slope of -1 (see red solid curve in the blue ellipse of Fig. 3). These conclusions are illustrated in Fig. 5 where the averaged value of Z error bar (ε_Z) is plotted as a function of the lander longitude (upper panel) and latitude (lower panel). The former is quite jittered due to geological features especially around longitude 135° (clearly visible in Fig. 4) but does not present any dependency to λ. In contrast, one can clearly see that the precision we can get on Z is proportional to the latitude of the lander, which is a function of the distance to spin axis r: the higher in latitude the lander, the more precise Z.

As a conclusion, our method should permit us to provide the third Z-coordinate of InSight with a precision (or error bar) of about 10 m after 2 days of operations. It is to mention that Digital Terrain Models of higher precision and spatial resolution have been derived from MEX-HRSC (Gwinner et al., 2010) and MRO-CTX/HiRISE (Kirk et al., 2008; Howington-Kraus et al., 2015) that would be used after landing so the results presented here represent a worst case.

7. Validation with previous landed missions

If the method described above takes into account the topography when computing the error bars of Z, the process by nature ignore the errors induced by the topography model approximation. Even if the model is based on very high precision altimeter data (at the level of few tens of centimeters), the interpolation process used to link the data points and deliver a continuous model of the surface of Mars induces systematic errors difficult to estimate. The resolution of the DSK topography model, i.e. the length of the plates, is in average ~0.5 km in the landing site region of InSight. This means that DSKs do not capture structures smaller than 500-m wide. In this section we test the accuracy of the method based on previous landed missions for which we find the estimated coordinates in the literature. These mission locations are shown on the map of Mars (Fig. 6). We apply our method to five of these missions whose coordinates are listed in Table 2.

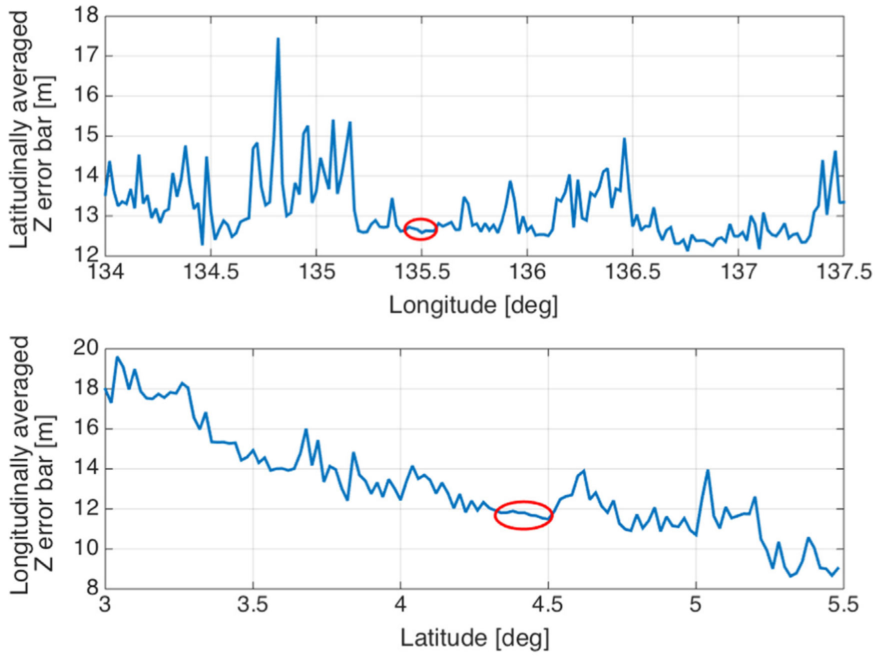

Fig. 5. Mean value of the error bar in Z (ε_Z) when averaging over the latitudes in the range of $[3^\circ : 5.5^\circ]$ (upper panel) and over the longitude in the range of $[134^\circ : 137.5^\circ]$ (lower panel). Values representative of the landing ellipse region are pointed out by the red ellipse. Effects of the big structures in the area have been damped a little bit by considering $\sigma_{Z_0} = 100$ m instead of the 3 km of the nominal scenario. (For interpretation of the references to color in this figure caption, the reader is referred to the web version of this paper.)

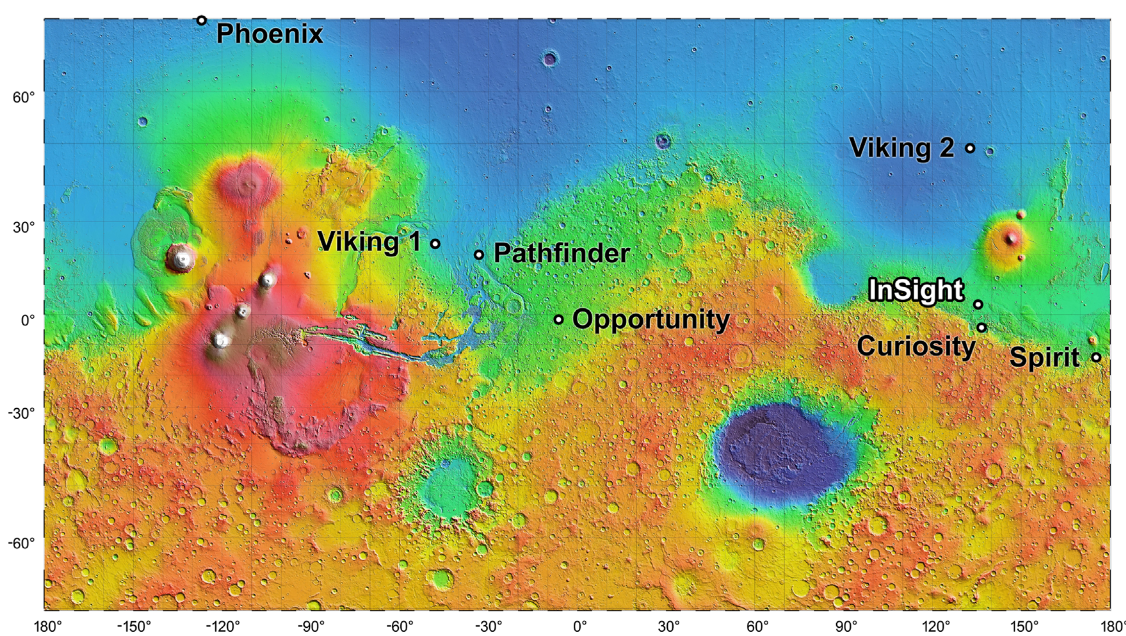

Fig. 6. Mars landed missions location (*NASA credit*).

Curiosity and Phoenix are not considered here because the former is moving and the latter did not communicate in direct-to-Earth. Spirit coordinates in Table 2 locate the rover when it got trapped in sandy soil before dying in 2009. Remaining motionless for hundreds of days, Spirit was still tracked from the DSN during this period. Between January and May 2012, Opportunity stopped moving for energy saving, becoming a quasi-equatorial fixed station communicating in X-band directly with the ground stations on Earth. Table 2 provides Opportunity coordinates during this period. The table also contains the Z estimates we get with our method. A comparison of our solutions (range of allowed Z from which the mean value and error bars of Table 2 have been inferred) with the estimates published by Kuchynka et al. (2014) is shown in Fig. 7. The reference values, in red in the figure, have been estimated by Kuchynka et al. (2014) along with the rotation parameters of Mars. They are the last ones that have been published.

Generally speaking, we see that all our solutions fall in the 3σ domain proposed by Kuchynka et al. (2014) except for Opportunity. Moreover all our solutions are much more precise than what is found in the literature (see Table 2), except for Viking Lander-2 for which the range of allowed Z according to the uncertainties in λ and r is almost twice the current uncertainty. In the latter case of Viking-2, no DTE Doppler data have been used, but only the low-

Table 2
Landers and rovers position estimates from Kuchynka et al. (2014) followed by the Z-coordinate inferred from them with our method.

Coordinate	Viking 1	Viking 2	Pathfinder	Opportunity	Spirit
Kuchynka et al. (2014)					
λ_0 (°)	-47.95137(fixed)	134.2803 ± 0.0001	326.74576 ± 0.00004	-5.35714 ± 0.0001	175.5271 ± 0.0001
r_0 (km)	3136.5188 ± 0.0002	2277.36 ± 0.02	3203.2057 ± 0.0001	3391.4868 ± 0.0002	3282.6785 ± 0.0001
Z_0 (km)	1284.556 ± 0.01	2500.14 ± 0.01	1109.20 ± 0.04	-132.02 ± 0.06	-855.54 ± 0.06
This study					
Z_{new} (km)	1284.5330 ± 0.0005	2500.1261 ± 0.016	1109.1685 ± 0.0003	-131.7644 ± 0.0086	-855.4185 ± 0.0003

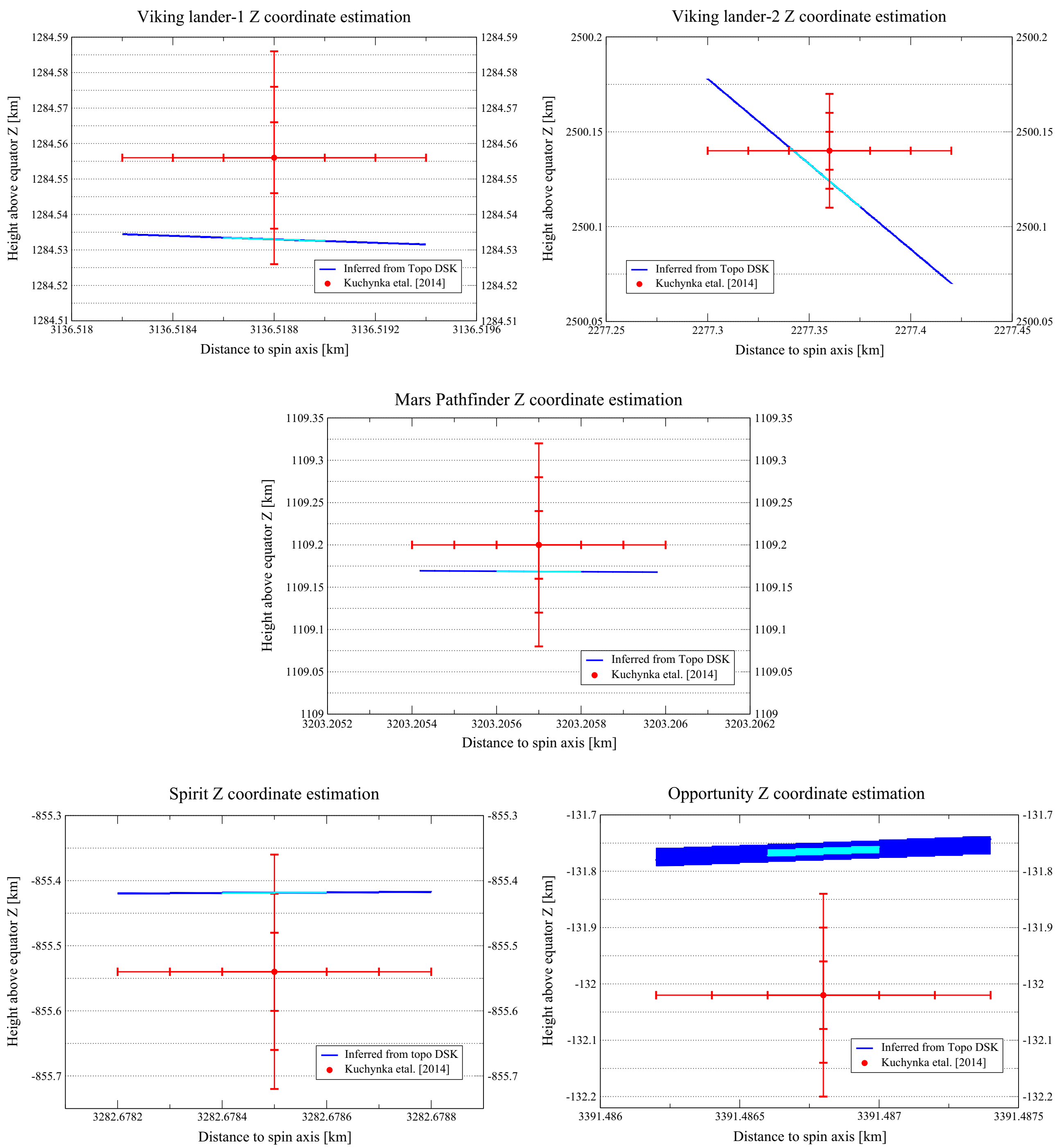

Fig. 7. Comparison between the current 1σ, 2σ, and 3σ estimates (red) of the previous NASA's landers and rovers locations and our estimates from the DSK-topography model and from the 1σ (cyan) and 3σ (dark blue) solutions of r and λ (Kuchynka et al., 2014). (For interpretation of the references to color in this figure caption, the reader is referred to the web version of this paper.)

accuracy-S-band range data explaining the very large uncertainty in r ($\sigma_{r_0} = 20$ m). As explained in the previous section, because of the ellipsoidal shape of Mars, the propagation of σ_r to ε_Z depends on the latitude of the lander and thus on the actual r value (as pointed out in the case of InSight with Fig. 5 lower panel). Given the latitude of Viking-2, the large uncertainty in Viking-2 r solution propagates to Z such that the latter evolves in a range of about the same amplitude: 2×20 m at 1σ (cyan in upper right panel of Fig. 7). The dependency between σ_r and ε_Z is clearly noticeable in the case of Viking-2 (slope on the top-right panel of Fig. 7), but it exists for every landers (negative slope in the northern hemisphere and positive in the southern one). Actually because of the high-latitude landing site of Viking-2 this dependency is damped with respect to the other landers for which this signature is barely visible only because of their 100 times better precision in r.

Opportunity's Z-coordinate is the worse determined by this method, with the largest error bar and the more biased with respect to the solution of Kuchynka et al. (2014). The large error bars are explained (as mentioned before) by the fact that Opportunity is the closest to the equator where the partial derivative of Z with respect to r tend to infinity, i.e. where a small variation (or uncertainty) in r will correspond to a very large variation (or uncertainty) in Z. As for the bias between our solution and the one of Kuchynka et al. (2014), the explanation certainly lies in the peculiar terrain where the rover was at the time of the radio-science campaign when its position has been determined. Indeed, as shown in Fig. 8, Opportunity was at "Greeley Haven", near the western rim of the Endeavour crater, motionless for power saving during the 2012 martian winter. We know and mentioned that the "low-resolution" topography model used should introduce systematic errors which should be more probable to exist in the vicinity of consequent structures like craters. We think thus that our bias should be due to the topography error increased by the proximity of the Endeavour crater. This hypothesis would also explain the accurate solution we get for Pathfinder, which is located in the ancient flood plain in Mars' northern hemisphere known as Ares Vallis (see Fig. 8). High-resolution maps of all the landers are available (Kirk et al., 2012) and could be used to test this assertion. These maps include the location of the landers and their elevation and the location of the rovers when they were stationary. In particular HiRISE stereo DEMs with 1 m elevation postings exist for Spirit and Opportunity (from the USGS Flagstaff web site) and these can be used with the location of the rover when they were tracked. This would substantially improve the elevation and the estimate could be compared to the MOLA estimate reported in Table 2.

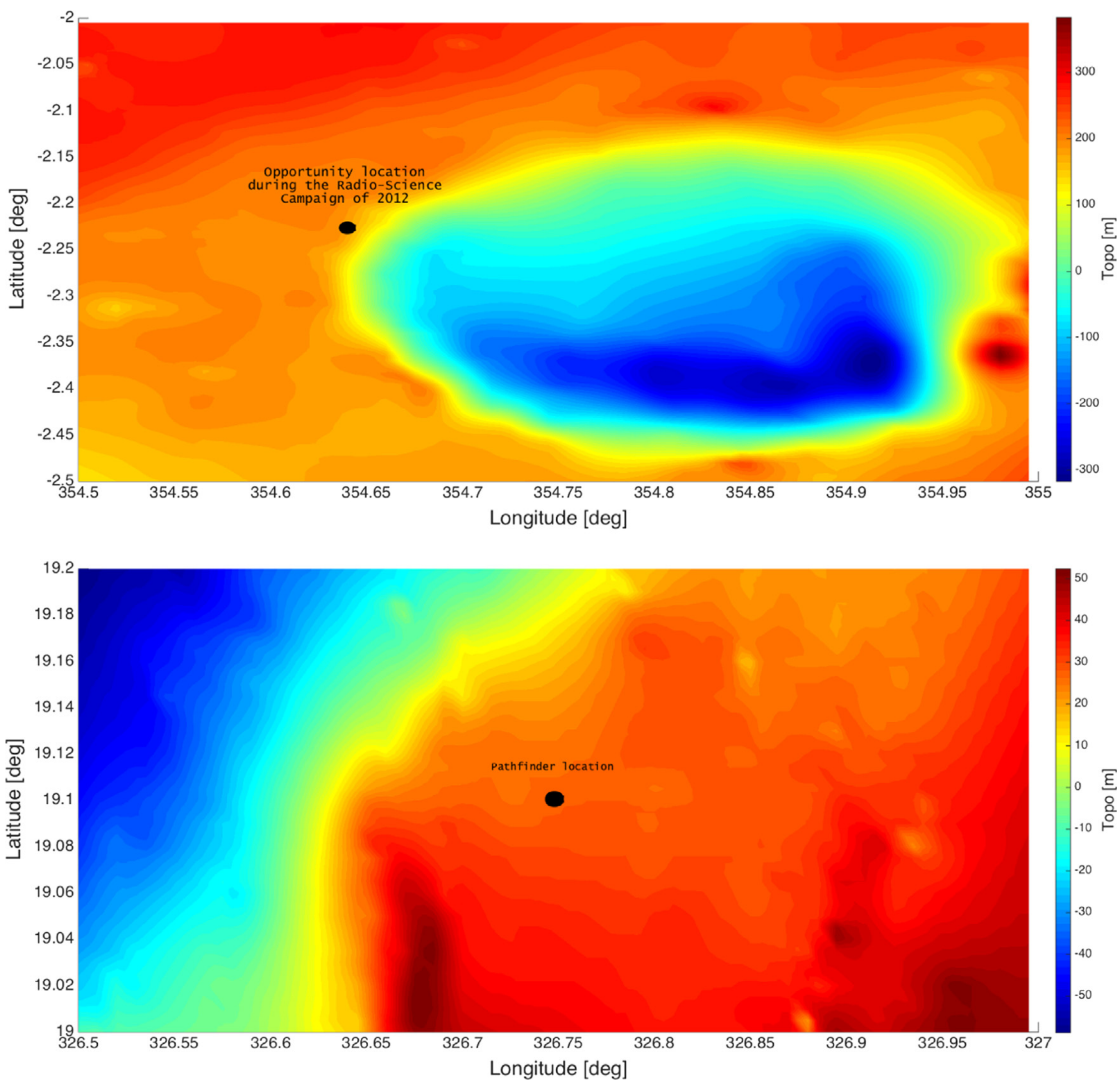

Fig. 8. Comparison of the Opportunity (upper panel) and the Pathfinder (lower panel) location topography to explain how accurate are the determination of their Z-coordinate. The MER is on the western rim of the Endeavour crater, whereas Pathfinder is in the middle of the Ares Vallis plain.

According to the MOLA's topography model, Viking 1 and 2 and Spirit last position reported in Table 2 are all in flat areas with few topographic variations (not shown here) giving some confidence about the accuracy of our *Z*-estimates for those three. InSight will land within the flat-lying Elysium Planitia, which is a smooth terrain with very few rocks in the highest-resolution images, for which our method should be quite accurate.

8. Conclusion

We proposed here a simple method to determine the coordinates of a landed probe with high precision and accuracy in a very short time after the starting of operations. The method consists of (1) first estimate the two in-equatorial plane coordinates of the lander from a couple of hours of Direct-to-Earth (DTE) Doppler tracking and (2) then, using these 1 m-precision-estimates, to determine the range of possible *Z*-coordinate laying the lander on the surface of the planet as predicted by a topography model. The method is applied to the selected landing ellipse of InSight, showing that the lander *Z*-coordinate should be estimated at the 10 m level (worst case) or better after two days of DTE Doppler tracking operations. This is more than two orders of magnitude better than the DTE Doppler solution alone. The precision on *Z* we get with this method depends on the latitude of the lander and on the flatness of the terrain, whereas the accuracy depends on the accuracy of the topography model used (which is also better in flat-smooth regions). We tested the method on the previous landed mission based on the MOLA digital elevation model in the NAIF-SPICE-DSK format, resulting in more precise *Z* solutions for all the probes considered except Viking 2 and with a likely more accurate solution for Pathfinder, Viking 1 and possibly Spirit and Viking 2. The landers and rovers coordinates could be further improved by using existing higher resolution maps.

Acknowledgment

The research carried out at the Jet Propulsion Laboratory was supported by an appointment to the NASA Post-doctoral Program at the Jet Propulsion Laboratory, administered by Oak Ridge Associated Universities through a contract with NASA. The author would like to thank Nat Bachman and the JPL-NAIF Group for help with the DSK as well as William Folkner, who suggested to do the study and gave useful advice for the completion of the paper. I thank T. Duxbury and M. Golombek for their insightful comments.

References

Folkner, W.M., Yoder, C.F., Yuan, D.N., Standish, E.M., Preston, R.A., 1997. Interior structure and seasonal mass redistribution of Mars from radio tracking of Mars Pathfinder. Science 278 (December), 1749–1751. http://dx.doi.org/10.1126/science.278.5344.1749.

Folkner, W.M., Asmar, S.W., Dehant, V., Warwick, R.W., 2012. The Rotation and Interior Structure Experiment (RISE) for the InSight mission to Mars. In: Lunar and Planetary Institute Science Conference Abstracts, Lunar and Planetary Institute Technical Report, vol. 43, March, p. 1721.

Golombek, M., Wigton, N., Bloom, C., Schwartz, C., Kannan, S., Kipp, D., Huertas, A., Banerdt, B., 2014. Final four landing sites for the InSight geophysical lander. In: Lunar and Planetary Science Conference, Lunar and Planetary Institute Technical Report, vol. 45, March, p. 1499.

Gwinner, K., Scholten, F., Preusker, F., Elgner, S., Roatsch, T., Spiegel, M., Schmidt, R., Oberst, J., Jaumann, R., Heipke, C., 2010. Topography of Mars from global mapping by HRSC high-resolution digital terrain models and orthoimages: characteristics and performance. Earth Planet. Sci. Lett. 294 (June), 506–519. http://dx.doi.org/10.1016/j.epsl.2009.11.007.

Howington-Kraus, E., Fergason, R.L., Kirk, R.L., Galuszka, D. , Redding, B., Theobald, M., Littlefield, E., Sutton, S., Fennema, A., Kipp, D., Otero, R.E., Golombek, M.P., 2015. High-resolution topographic mapping supporting selection of NASA's next Mars landing sites. In: Lunar and Planetary Science Conference, Lunar and Planetary Science Conference, vol. 46, March, p. 2435.

Kirk, R.L., Howington-Kraus, E., Rosiek, M.R., Anderson, J.A., Archinal, B.A., Becker, K. J., Cook, D.A., Galuszka, D.M., Geissler, P.E., Hare, T.M., Holmberg, I.M., Keszthelyi, L.P., Redding, B.L., Delamere, W.A., Gallagher, D., Chapel, J.D., Eliason, E. M., King, R., McEwen, A.S., 2008. Ultrahigh resolution topographic mapping of Mars with MRO HiRISE stereo images: meter-scale slopes of candidate Phoenix landing sites. J. Geophys. Res. (Planets) (November). http://dx.doi.org/10.1029/2007JE003000 113:E00A24.

Kirk, R.L., Howington-Kraus, E., Archinal, B.A., Keszthelyi, L.P., Golombek, M.P., 2012. Landers and rovers need high resolution topographic maps: lessons from the NASA Mars exploration program. In: LPI Contributions, No. 1679, June 2012, p. 4361.

Kuchynka, P., Folkner, W.M., Konopliv, A.S., Park, R.S., Le Maistre S., Dehant, V., 2014. New constraints on Mars rotation determined from radiometric tracking of the Opportunity Mars Exploration Rover. Icarus, 229: 340–347, ISSN 0019-1035, http://dx.doi.org/10.1016/j.icarus.2013.11.015⟨http://www.sciencedirect.com/science/article/pii/S0019103513004879⟩.

Le Maistre, S., Rosenblatt, P., Rivoldini, A., Dehant, V., Marty, J-C., Karatekin, Ö., 2012. Lander radio science experiment with a direct link between Mars and the Earth. Planet. Space Sci. 68 (July (1)), 105–122, ISSN 0032-0633. http://dx.doi.org/10.1016/j.pss.2011.12.020.

Smith, D.E., Zuber, M.T., Frey, H.V., Garvin, J.B., Head, J.W., Muhleman, D.O., Pettengill, G.H., Phillips, R.J., Solomon, S.C., Zwally, H.J., Banerdt, W.B., Duxbury, T. C., Golombek, M.P., Lemoine, F.G., Neumann, G.A., Rowlands, D.D., Aharonson, O., Ford, P.G., Ivanov, A.B., Johnson, C.L., McGovern, P.J., Abshire, J.B., Afzal, R.S., Sun, X., 2001. Mars Orbiter Laser Altimeter: Experiment summary after the first year of global mapping of Mars. J. Geophys. Res. 106 (October), 23689–23722. http://dx.doi.org/10.1029/2000JE001364.